Environmental Resources Research
Vol. 7, No. 1, 2019

GUASNR

Spatio-temporal distribution of off-shore ships in the Pars Special Economic Energy Zone based on satellite imagery

Q. Ashournejad[1], F. Amiraslani[2*], M. Kiavarz Moghadam[3], A. Toomanian[4]
[1]Ph.D candidate of Remote Sensing and GIS, Department of Remote Sensing and GIS, Faculty of Geography, University of Tehran, Tehran, Iran
[2]Associate Professor of Remote Sensing and GIS, Department of Remote Sensing and GIS, Faculty of Geography, University of Tehran, Tehran, Iran
[3]Assistant Professor of Remote Sensing, Department of Remote Sensing and GIS, Faculty of Geography, University of Tehran, Tehran, Iran
[4]Assistant Professor of GIS, Department of Remote Sensing and GIS, Faculty of Geography, University of Tehran, Tehran, Iran

Received: March 2018 ; Accepted: December 2018

Abstract

Special Economic Zones (SEZs) are areas controlled by specific legislations so as to attain economic prosperity. These zones are commonly established and controlled by government officials and are primarily characterized by growing population and developing transport infrastructure. One relevant case is the Pars Special Economic Energy Zone (PSEEZ) situated in the south of Iran, on the northern shores of the Persian Gulf. This particular zone has been formed to extract, refine, and export gas. The coast of the Persian Gulf has brought on further expansions in sea transportation, thereby increasing shipping activities in the area. The chief mode of shipping goods and materials in the PSEEZ is Maritime transportation. Identification of areas where traffic is carried out requires the collection of spatial data of ships. These spatial data are utilized in several applications for modeling of marine ecosystem. The central purpose of this research is to procure spatial data required for the PSEEZ using optical remote sensing images. Thus, Landsat-8 and Sentinel-2 images spanning from 2013 to 2018 were incorporated to identify ships in the study area. The threshold-based method was implemented for detecting the ships using infrared bands of 172 images, upon which a total of 3361 ships were identified. The map of areas affected by ship traffic was prepared using Hot Spot analysis. The results specify that more than 80 square kilometers of the marine environment has been affected by ship traffic during the years 2013- 2018.

***Keywords*: Maritime transportation, Ship detection, Remote sensing, GIS, PSEEZ**

***** Corresponding author; amiraslani@ut.ac.ir

Introduction

Special Economic Zones (SEZs) are set up by governments to support economic activities. Establishing international trades, producing goods, transferring technology, generating productive employment, and encouraging domestic and foreign investment are the major reasons behind the creation of these areas (Hejazi *et al.*, 2015). The Pars Special Economic Energy Zone (PSEEZ) of southern Iran is a prime example of such areas, which has recently become a national and transnational zone. A variety of activities take place in the area such as extraction, exploitation, refinement and export of gas (Talebian *et al.*, 2008). The development of the PSEEZ has engendered further operations including the establishment and construction of petrochemical refineries, followed by the attraction of population and development of transportation infrastructures in the region (Figure 1). The location of the PSEEZ along the Persian Gulf coast and its access to free waters provide context for the development of maritime transportation (Chengjin *et al.*, 2018). This mode of transportation is commonly used for the transportation of goods and materials in the PSEEZ.

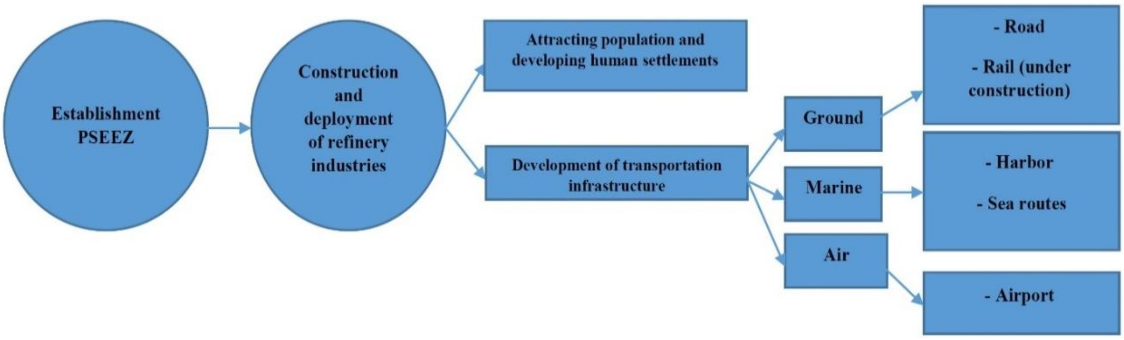

Figure 1. Establishment of the PSEEZ and the development of its related infrastructure

Disregard of ecological rules and regulations in the development of harbors and ship traffic are bound to affect marine ecosystems (Wei *et al.*, 2018). The major problems with ship traffic are air, noise and oil pollution. Waste, sewage drainage, ballast water, toxic substances are among other predicaments that can be mentioned (Andersson *et al.*, 2016; Peng *et al.*, 2015). An example of the impacts of ship traffic in the study area is the rather high concentration of heavy metals in waters of this region (Dobaradaran *et al.*, 2018). Ships, in particular tankers, discharge ballast water when entering the area in accordance with sea safety regulations. The literature shows that in the long run, ballast water can and will most likely change the quality of chemicals in marine environments, while also affecting human health and the marine ecosystem. The subsequent entry of invasive species inflicts heavy damages to sensitive coastal and marine ecosystems. Therefore, permanent monitoring and ballast water treatment before discharge are crucial to the preservation of marine environmental health.

In order to locate areas affected by ships, spatial and temporal traffic information must be acquired and extracted so as to generate a map of affected zones. In addition to modelling the marine ecosystems, the map could be employed in a wide range of applications including sea safety, marine spatial planning, illegal fishing management, marine defense security, piracy, unauthorized immigration and control of borders (Kanjir *et al.*, 2018). Remote sensing is one of the most valuable tools for ship detection and identification which grants the user access to several features including global coverage, appropriate spatial and temporal resolution as well as easy and free access to a large corpus of data (Marino *et al.*, 2015; Ouellette and Getinet, 2016; Cozzolino and Lasta, 2016). Although Synthetic Aperture Radar (SAR) data is still the leading technology for ship detection, optical remote sensing images are rapidly becoming famous. The ongoing developments and advancements in the temporal resolution of optical images have encouraged the prevalent use of optical images as a means of ship detection (Kanjir *et al.*, 2018). Various image datasets have emerged in this regard, the most notable of which are the Landsat-8 and Sentinel-2 images, which have significant potential for ship detection applications (Wang *et al.*, 2017).

The purpose of this research is to detect ships in the PSEEZ to provide a map of areas affected by ship traffic using remote sensing data (Landsat-8 and Sentinel-2) for a period of 5 years from 2013 to 2018.

Materials

Study area

PSEEZ is the largest special economic-led zone for oil, gas and petrochemical industries throughout the world (Figure 2). The area was established in 1998 to extract oil and gas resources from the South Pars field and carry out economic activities in the city of Asaluyeh, Bushehr Province (PSEEZ, 2018).

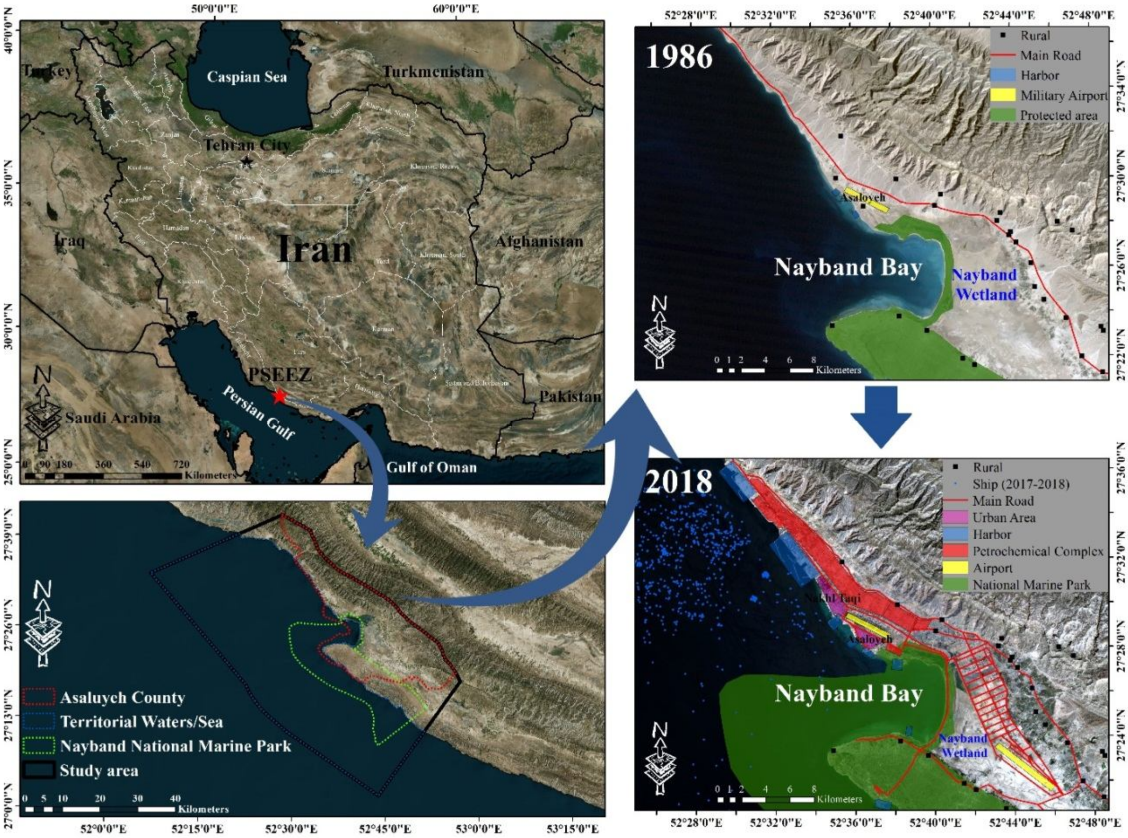

Figure 2. The study area (PSEEZ), and infrastructure of the PSEEZ before its establishment in 1986 and after its establishment in 2018

In the past, the inhabitants primarily resorted to fisheries and agricultural activities as their main source of income, however, the area is now surrounded by a large number of oil and gas factories or industrial facilities. The region, extending to 22,500 hectares in area, was tagged as the Nayband protected area in 1978. The Nayband protected area, along with parts of Persian Gulf, with an approximate area of 49815 ha, were registered as the first Iranian Marine National Park in 2003 (Owfi and Owfi, 2018). The presence of coral reefs, mangrove forests, rocky beaches, and real estuaries make this area one of the most diverse and beautiful coastal ecosystems in the world. The area also enjoys a variety of aquatic species, marine mammals such as dolphins and whales, endangered reptiles, such as the green and eagle tip turtle and different kinds of aquatic birds (Zahed *et al.*, 2010; Owfi and Owfi, 2018).

Based on the findings of surveys, the Nayband area is in several ways exposed to the threat of oil and gas contaminants (Dialogue and Development in Iran, 2013). Most of these threats are from maritime transportation in the PSEEZ, including the Pars port complex and the transit route of oil tankers, which upon passing the Strait of Hormuz make way towards Lavan Island, Asalouyeh, Bandar Taheri, Kharg Island, Khuzestan oil fields and in general the Persian Gulf oil fields. Experiences from innumerable parts of the world has shown that such cases are bound to occur as the universal effects of the development of oil and gas industries. In the absence of proper management, this could lead to long-term negative impacts on the animal and plant communities and the surrounding natural settings. Therefore, the establishment of effective systems for monitoring and controlling the status of the region in different environmental dimensions is of utmost importance (Torkianfar *et al.*, 2010).

The present study investigates 200,000 hectares (2000 square kilometers) of the Persian Gulf area, considered to be Iran's territorial waters, as well as the Southern PSEEZ.

Data Sources

A total of 27 images from Landsat-4 and 5 were used to assess the status of ship traffic prior to the establishment of the PSEEZ, and afterwards, ship traffic routes in the PSEEZ from 2013 to 2018 were determined using 172 Landsat-8 and Sentinel-2 images. Landsat-8 has 11 spectral bands that cover the range of visible to infrared thermal wavelengths. The visible, infrared, and short-wave infrared ranges include 8 bands with a resolution of 30 meters. Two thermal infrared bands have a spatial resolution of 100 meters, which were resampled to 30 meters. The Landsat-8 Panchromatic Band with a resolution of 15 meters was obtained with the aim of improving the quality and quantity of visible bands (NASA, 2017).

The European Space Agency's Copernicus program, aiming to produce consistent and high quality ground observation data on a global scale has launched a new family of earth observation satellites called the Sentinel (Castro Gomez, 2017). Each Sentinel satellite has at least two satellites with full coverage of Earth, which provides the required data for the Copernicus program. Sentinel-2 is one of the multispectral satellites of this program, which covers visible, near-infrared, and short-wave infrared ranges with 13 bands, 4 with a resolution of 10 m, 6 with a resolution of 20 m, and the remaining 3 bands with a resolution of 60 m (ESA 2017). Landsat 8 has a 16-day revisit time, whereas the Sentinel-2A & 2B have a combined 5-day revisit time (Li and Roy, 2017).

Figure 3 shows an example of a ship detected by these images. The figure represents a ship in the study area and includes the true color combination (bands 2, 3, 4) and the infrared band from both satellites (spatial resolution of Sentinel-2 and Landsat-8 is 10 and 30 m respectively). Also, the panchromatic band and the true color combination (bands 2, 3, 4) were integrated with Landsat-8 panchromatic bands in order to improve the pixels of visible bands of Landsat-8 from 30 meters to 15 meters. The figure clearly shows the difference between Landsat-8 and Sentinel-2 for the detection of ships. The two satellites receive 7 to 8 images per month from the entire study area.

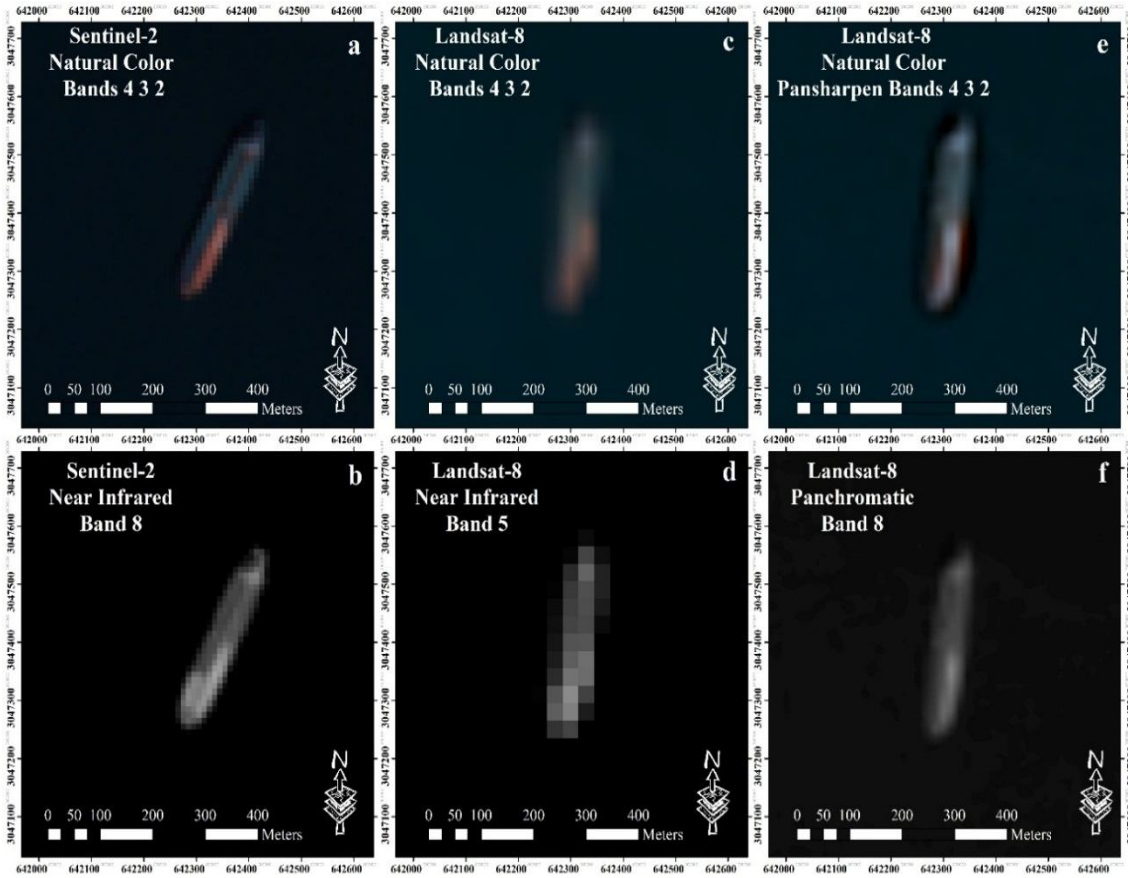

Figure 3. An example of a ship from the images of Sentinel-2 and Landsat 8, received on 2016.02.15 from the study area. **a**: True color combination (4, 3, 2) of Sentinel-2 with a resolution of 10 meters; **b**: near-infrared (Band 8) of Sentinel-2 with a resolution of 10 meters; **c**: True color combination (bands 4,3, 2) of Landsat-8 with a resolution of 30 m; **d**: near-infrared (band 5) of Landsat-8 with a resolution of 30 meters; **e**: True color combination (Landscape 4-band 4) of Landsat-8 combined with Landsat-8 panchromatic band to improve spatial resolution from 30 meters to 15 meters; **f**: Landsat-8 panchromatic band with a resolution of 15 meters

Methods

The present study sought to use the most common methods for identifying ships based on satellite imagery, primarily due to the fact that ships are brighter than their surroundings. The threshold method, as one of the classic and widely used methods for identifying ships, divides the image into pieces based on the threshold value selected on the histogram. This method is particularly suitable for situations with smooth sea levels or high contrast between ship targets and sea background. The threshold was selected experimentally (Kanjir *et al.*, 2018). After comparing Landsat-8 and Sentinel-2 bands, the near-infrared band (Landsat-8 band 5 and Sentinel-2 band 8) was selected for ship detection using the threshold method. The next stage was to recognize whether the object was a ship or not. This step aims to remove the misclassified items obtained from the previous step (Bi *et al.*, 2010). One common manner by which researchers identify misclassified items is the use of geometric characteristics such as size (length, width, and length to width ratio) or a combination of spectral and geometric properties (Kanjir *et al.*, 2014; Kanjir *et al.*, 2018). The present study employed geometric characteristics to make the final decision in detecting ships. Ultimately, the identified ships were visually controlled and evaluated.

Hotspot analysis was used to determine the areas affected by ship traffic in GIS environment (Zhang *et al.*, 2017). To conduct this analysis on ships identified from satellite imagery, the study area was divided into 400 × 400 meters nets of rectangular cells (Fishnet), wherein the number of ships identified in each net was connected to its attribute value. This analysis considers each net along with its neighboring nodes. If a net has high values, it is deemed to be important, otherwise it may not be statistically significant to be leveled as a hot spot. In order to be considered a hot spot and statistically significant, both the net and its neighbors must have high values (Huang *et al.*, 2013). Hot Spot analysis calculates the Getis-Ord Gi statistic for all nets using Equation 1 (Yu and Yi, 2014; Yunus *et al.*, 2015; Yingjie *et al.*, 2017):

$$G_i^* = \frac{\sum_{j=1}^{n} w_{i,j} * x_i - \bar{X} * \sum_{j=1}^{n} w_{i,j}}{S * \sqrt{\frac{\left[n \sum_{j=1}^{n} w_{i,j}^2 - \left(\sum_{j=1}^{n} w_{i,j}\right)^2\right]}{n-1}}} \quad (1)$$

where n is the total number of nets, x_i is the attribute value for j and $w_{i,j}$ is the spatial weight between i and j. $\bar{X}$, and S are calculated according to Equations 2 and 3:

$$\bar{X} = \frac{\sum_{j=1}^{n} x_j}{n} \quad (2)$$

$$S = \sqrt{\frac{\sum_{j=1}^{n} x_j^2}{n} - (\bar{X})^2} \quad (3)$$

Results and Discussion

Following the separation of sea from land and the removal of clouds from all images, the threshold method was applied. No ships were detected in the 27 images from 1987, 1990, and 1991, prior to the establishment of the PSEEZ. Subsequently, the threshold method was applied to 172 images from 2013 to 2018, after the establishment of the PSEEZ, and the results are presented in Figure 4. The results (Table 1 and Figure 6) show an increase in the presence of ships from 2013 to 2016 from an average of 15 ships per image to 31 ships. The increase peaked in 2016. A significant drop is seen in the presence of ships in the studied area in 2017 and 2018 (an average of 14 and 11 ships per image). During these years the presence of ships in the east of the study area and near the Nayband bay had increased. Furthermore, surfaces affected by the traffic of ships were determined by analyzing hot spots on identified ships (Figure 5). The results (Table 1 and Figure 6) indicate that more than 80 square kilometers of the study area is affected by the traffic of each ship per year.

The largest affected areas in 2014, 2018, 2016, and 2017 were 140, 136.48, 117.28 and 100.96 square kilometers, respectively. Also, the lowest affected areas in 2013 and 2015 were 80.48 and 93.12 square kilometers, respectively. These results were obtained at 90, 95, and 99 percent confidence intervals. Taking into account the ships identified during the entire period from 2013-2018, approximately 144.48 square kilometers of the study area is affected by ship traffic ships, of which 107.52 square kilometers are within a 99 percent confidence interval.

Table 1. Results of identified ships and hot spots analysis from 2013 to 2018

Year	Number of images	Number of ships	Mean number of ships per image	Area of hot spots	Area of hot spots with 90% confidence	Area of hot spots with 95% confidence	Area of hot spots with 99% confidence
2013	15	218	15	80.48	45.6	0.32	34.56
2014	17	330	19	140	86.08	0.32	53.6
2015	25	586	23	93.12	29.76	0	63.36
2016	40	1255	31	117.28	29.28	15.68	72.32
2017	46	658	14	100.96	36.64	0	64.32
2018	29	314	11	136.48	86.72	0.32	49.44
All	172	3361	20	144.48	14.24	22.72	107.52

(Units for columns 5 to 8: sq. Km)

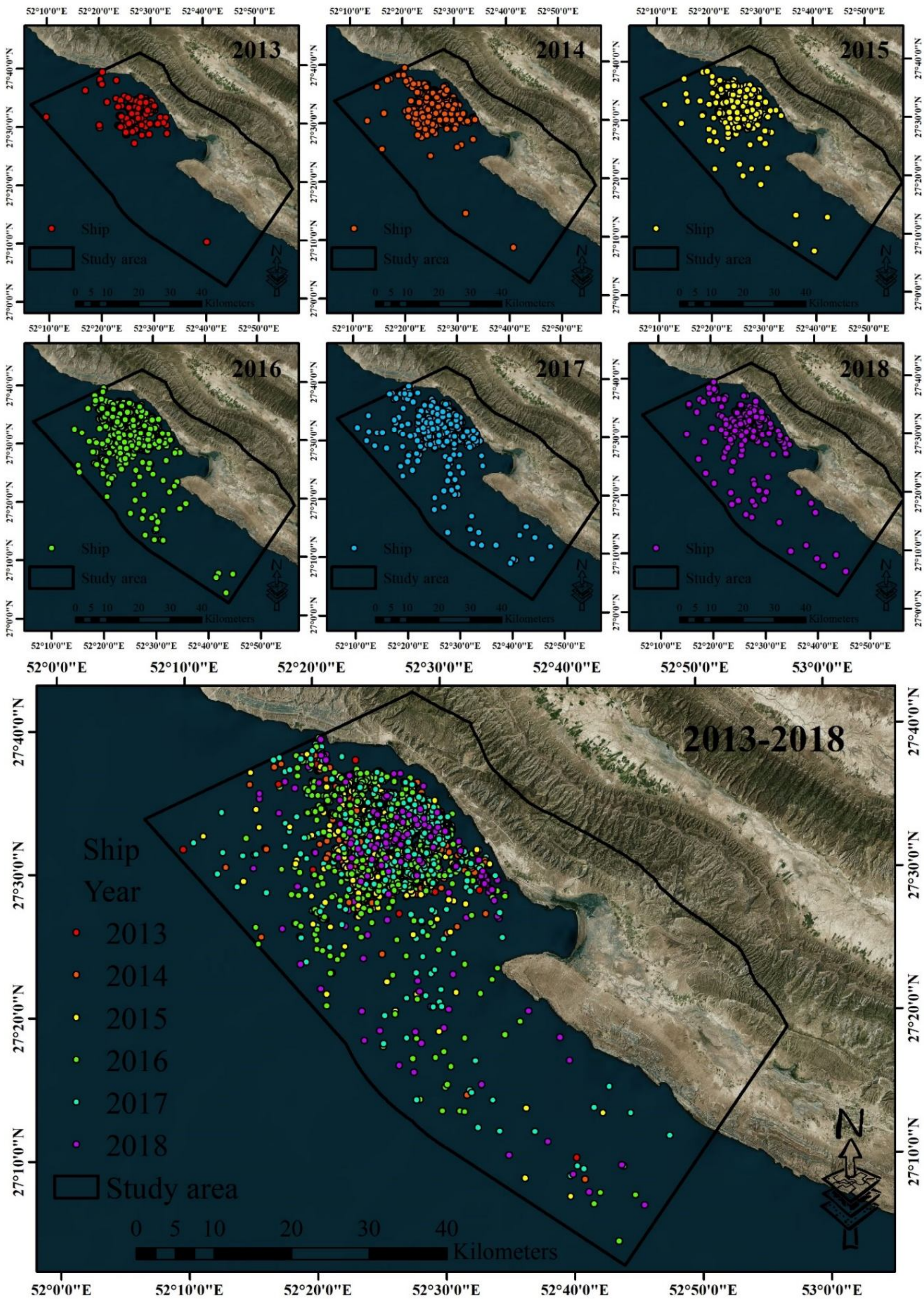

Figure 4. The ships identified using Landsat-8 and Sentinel-2 images from 2013 to 2018

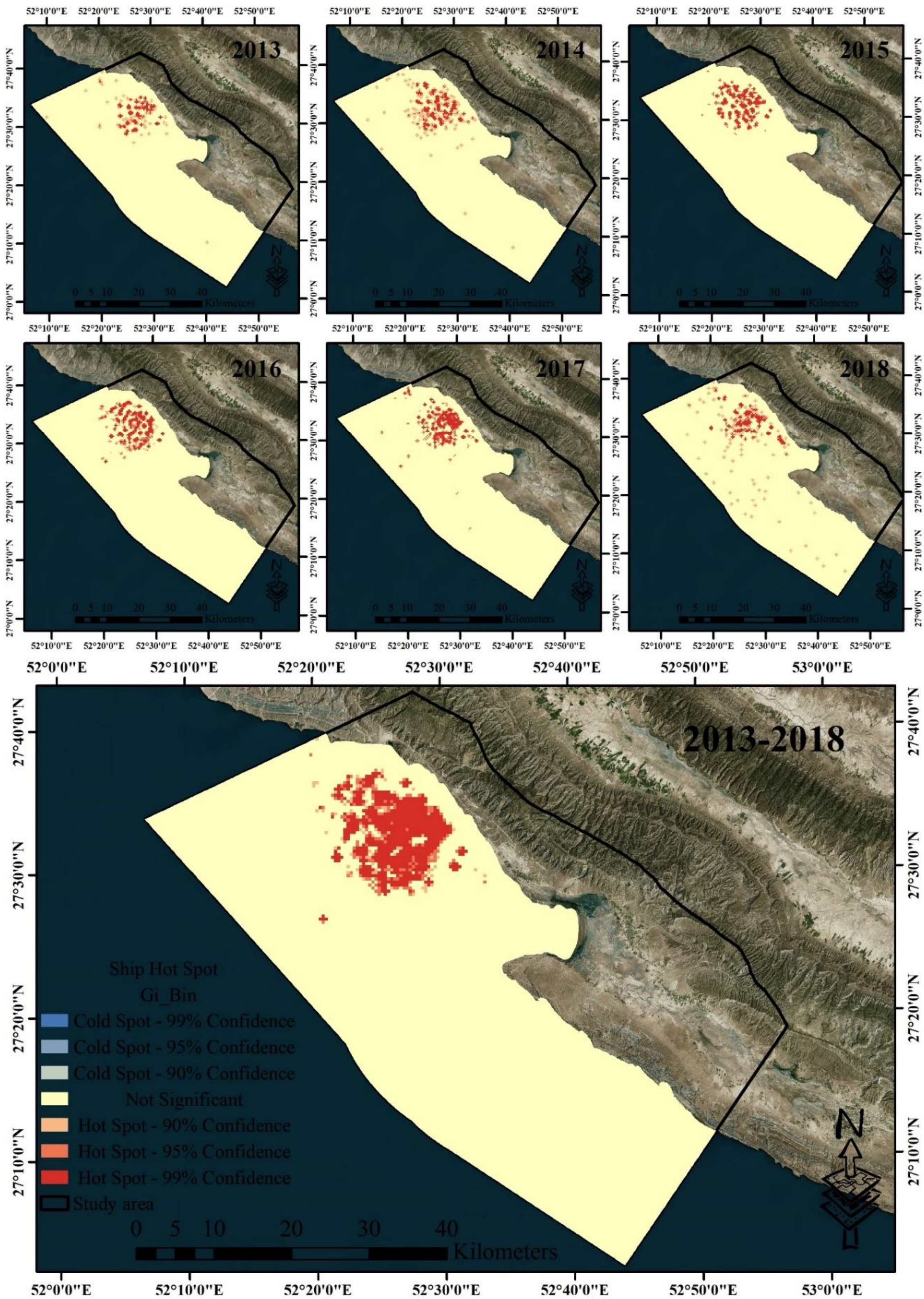

Figure 5. Analysis results of hot spots (waters affected by the ship traffic from 2013 to 2018)

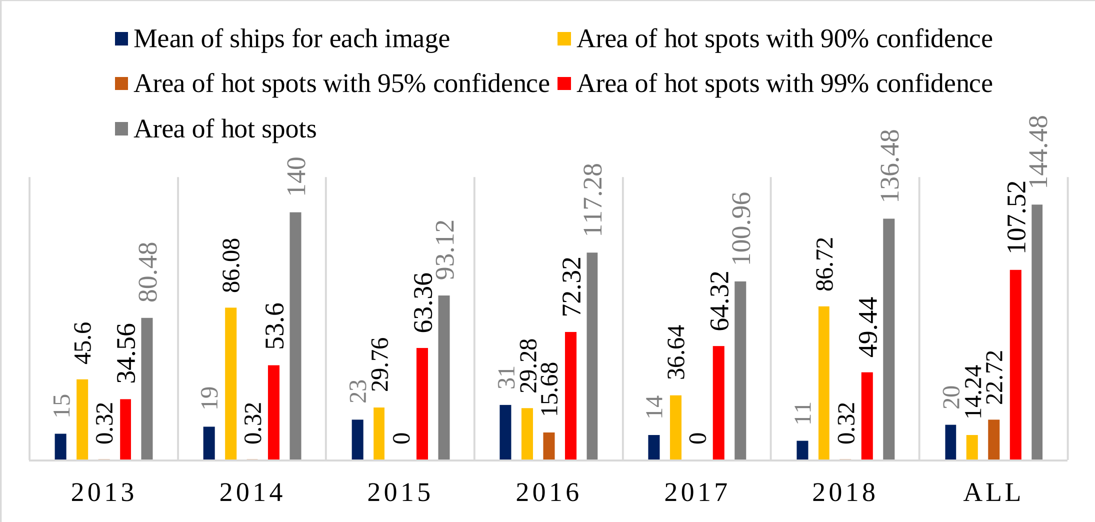

Figure 6. Results of identified ships and analysis of hot spots from 2013 to 2018

Results indicate a significantly high ship traffic in the majority of the study area after the establishment of the PSEEZ. The amount of traffic versus the capacity of the region in producing oil and gas is normal. According to the latest report, exports of gas condensates and non-oil products of the region reached 2 million 684 thousand and 251 tons (PSEEZ, 2018). The regular monitoring of ship traffic and planning of transit routes can play a significant role in preserving marine ecosystems in the region. This research is the first of its kind to focus on spatial and temporal distribution of ship traffic in the PSEEZ. The majority of research solely refer to the pollution caused by ships in the region, and thus an investigation into the correlation between ship traffic and pollution was called for. The results of this study reaffirmed the efficiency of remote sensing in ship identification, however, certain limitations were also identified. One of the limitations of using remote sensing data in this study was the lack of access to images that cover all the days of the year for the given period. This could be resolved to a great extent by combining data from different sensors and increasing the number of remote sensing satellites. Other notable constraints include the dependence of optical remote sensing images on atmospheric conditions. This limitation can also be solved by using radar data along with optical data. The visual control and evaluation of ships identified using the threshold method increased the time needed to prepare a spatial database. By providing automatic detection systems for ships, it is possible to reduce the time needed to prepare a database and perform on-time analysis.

Conclusion

The results of our research indicate that remote sensing images are effective in identifying ships using GIS for spatial analysis. Certain directions for future research are as follows:

Since the impact of ships on marine ecosystem varies according to the type of ship (cargo, tanker, passenger, and fishing), it is suggested that future investigations identify ships based on type and incorporate relevant spatial analyses in GIS.

We recommended that in future, studies focus on using Sentinel-1 radar images alongside Landsat-8 and Sentinel-2 data. These data are the latest radar images for remote sensing applications that provide C band images during day and night and in various weather conditions. Independence from atmospheric conditions is one of the benefits of Sentinel-1 radar data, compared to Landsat-8 and Sentinel-2 optical images. In addition, the use of Sentinel-1 images will increase the number of available images from 8 to 13 images per month.

It is also recommended that the results of this research be used to identify the impact of ships on biodiversity as an ecosystem service. By providing a biodiversity map, it is possible to determine the extent of the impact of ship traffic and in turn take measures to preserve various species in the study area.

Conflict of Interest

The authors declare that they have no conflict of interest.

References

Andersson, K., Brynolf, S., Lindgren, J.F., and Wilewska-Bien, M. 2016. Shipping and the Environment: Improving Environmental Performance in Marine Transportation. 1st ed. Berlin: Springer Press.

Bi, F., Liu, F., and Gao, L. 2010. A hierarchical salient-region based algorithm for ship detection in remote sensing images. Advances in Neural Network Research and Applications. Springer, Berlin Heidelberg, 729–738.

Castro Gomez, M.G. 2017. Joint use of Sentinel-1 and Sentinel-2 for land cover classification: a machine learning approach. Master of Science (MSc) Thesis, Lund University.

Chengjin, W., Peiran, Ch., and Yunhao, Ch. 2018. The identification of global strategic shipping pivots and their spatial patterns. Journal of Geographical Sciences, 28(9): 1215-1232.

Cozzolino, E., and Lasta, C.A. 2016. Use of VIIRS DNB satellite images to detect jigger ships involved in the Illex argentines fishery. Remote Sensing Applications: Society and Environment, 4: 167–178.

Dialogue and Development in Iran: Building Multi-stakeholder Alliances (Asalouyeh Project), 2013. Newsletter. 3 (In Persian).

Dobaradaran, S., Soleimani, F., Nabipour, I., Saeedi, R., and Mohammadi, M.J. 2018. Heavy metal levels of ballast waters in commercial ships entering Bushehr port along the Persian Gulf. Marine Pollution Bulletin, 126: 74-76.

ESA. (2017). Sentinel Online; Radiometric Resolutions. Cited at: https://earth.esa.int/web/sentinel/user-guides/sentinel-2-msi/resolutions/radiometric

Hejazi, N., Fazel, R., and Vahida, F. 2015. Impacts of Economic Development of Assaluyeh on Quality of Life (by Industrial Development Approach). The Socio Cultural Strategy Journal, 4(14): 87-114 (In Persian).

Huang, D.Zh., Hu, H., and Li, Y.Zh. 2013. Spatial Analysis of Maritime Accidents Using the Geographic Information System. Transportation Research Record, 2326(1): 39-44.

Kanjir, U., Greidanus, H., and Oštir, K. 2018. Vessel detection and classification from spaceborne optical images: A literature survey. Remote Sensing of Environment. 207, 1-26.

Kanjir, U., Marsetič, A., Pehani, P., and Oštir, K. 2014. An automatic procedure for small vessel detection from very-high resolution optical imagery. In: 5th Geographic Object-Based Image Analysis Conference (GEOBIA). 4.

Li, J., and Roy, D.P. 2017. A Global Analysis of Sentinel-2A, Sentinel-2B and Landsat-8 Data Revisit Intervals and Implications for Terrestrial Monitoring. Remote Sensing. 9(9), 902.

Marino, A., Sanjuan-Ferrer, M.J., Hajnsek, I., and Ouchi, K. 2015. Ship Detection with Spectral Analysis of Synthetic Aperture Radar: A Comparison of New and Well-Known Algorithms. Remote Sensing, 7(5): 5416-5439.

NASA. 2017. Spectral Response of the Operational Land Imager In-Band, Band-Average Relative Spectral Response. Data downloads available. Cited at: https://landsat.gsfc.nasa.gov/preliminary-spectral-response-of-the-operational-land-imager-in-band-band-average-relative-spectral-response/

Ouellette, W., and Getinet, W. 2016. Remote sensing for marine spatial planning and integrated coastal areas Management: Achievements, challenges, opportunities and future prospects. Remote Sensing Applications: Society and Environment, 4: 138-157.

Owfi, R.E., and Owfi, F. 2018. Ecological study of Harra forests in the Nayband protected area at Bushehr province, Iran. International Journal for Research in Agricultural And Food Science, 4(6): 1–8.

Peng, C., Zhao, X., and Liu, G. 2015. Noise in the Sea and Its Impacts on Marine Organisms. International Journal of Environmental Research and Public Health, 12(10): 12304-12323.

PSEEZ, 2018. About PSEEZ Field. Retrieved July 26, 2018, from. http://www.pseez.ir/en/home

Talebian, A., Fazeli, M., and Daqaqeleh, A. 2008. The Social Impact Analysis of Development of Oil and Gas Industries in Asaluyeh. Journal of Social Science, 33: 55-75 (In Persian).

Torkianfar, F., Jafari, H.R., and Sadeghpour, A.H. 2010. Endangerment Survey of Construction Activities on Shore Line. Journal of Environmental studies. 35(52), 43-54 (In Persian).

Wang, Q., Blackburn, G.A., Onojeghuo, A.O., Dash, J., Zhou, L., Zhang, Y., and Atkinson, P.M. 2017. Fusion of Landsat 8 OLI and Sentinel-2 MSI Data. IEEE Transactions on Geoscience and Remote Sensing, 55(7): 3885–3899.

Wei, S., Cheng, Ch., and Lei, W. 2018. Spatial function regionalization and governance of coastal zone: A case study in Ningbo City. Journal of Geographical Sciences, 28(8): 1167–1181.

Yingjie, L., Liwei, Zh., Junping, Y., Pengtao, W., Ningke, H., Wei, Ch., and Bojie, F. 2017. Mapping the hotspots and coldspots of ecosystem services in conservation priority setting**.** Journal of Geographical Sciences, 27(6): 681-696.

Yu, Y., and Yi, L. 2014. Spatio-temporal analysis of urbanization and land and water resources efficiency of oasis cities in Tarim River Basin. Journal of Geographical Sciences, 24(3): 509-525.

Yunus, A., Dou, J., and Sravanthi, N. 2015. Remote sensing of chlorophyll-a as ameasure of red tide in Tokyo Bay using hotspot analysis. Remote Sensing Applications: Society and Environment, 2: 11–25.

Zahed, M.A., Rouhani, F., Mohajeri, S., Bateni, F., and Mohajeri, L. 2010. An overview of Iranian mangrove ecosystems, northern part of the Persian Gulf and Oman Sea. Acta Ecologica Sinic, 30(4): 240–244.

Zhang, L., Meng, Q., and Fwa, T.F. 2017. Big AIS data based spatial-temporal analyses of ship traffic in Singapore port waters. Transportation Research Part E: Logistics and Transportation Review. In Press.